# Human influence increases the likelihood of extremely early cherry tree flowering in Kyoto

ENVIRONMENTAL RESEARCH
LETTERS

LETTER • OPEN ACCESS

# Human influence increases the likelihood of extremely early cherry tree flowering in Kyoto

To cite this article: Nikolaos Christidis *et al* 2022 *Environ. Res. Lett.* **17** 054051

ENVIRONMENTAL RESEARCH
LETTERS

CrossMark

OPEN ACCESS

RECEIVED
7 March 2022

REVISED
11 April 2022

ACCEPTED FOR PUBLICATION
29 April 2022

PUBLISHED
16 May 2022



LETTER

# Human influence increases the likelihood of extremely early cherry tree flowering in Kyoto

Nikolaos Christidis[1,*], Yasuyuki Aono[2] and Peter A Stott[1]

[1] Met Office Hadley Centre, FitzRoy Road, Exeter EX1 3PB, United Kingdom
[2] Osaka Metropolitan University, Graduate School of Agricultural Science, Sakai 599-8531, Japan
* Author to whom any correspondence should be addressed.

E-mail: nikos.christidis@metoffice.gov.uk

Keywords: climate change attribution, climate change impacts, phenological changes

Supplementary material for this article is available online

## Abstract

The full flowering of Kyoto's cherry trees in 2021 was observed on the 26th of March, the earliest date recorded in over 1200 years. An early shift of the flowering season is consistent with Kyoto's warming climate and could have serious repercussions for the local economy. It is therefore crucial to assess how human activity impacts flowering dates and alters the likelihood of extremely early flowering. To make this assessment, our study combines a risk-based attribution methodology with a phenological model that estimates full flowering dates from daily temperature data. We employ 14 state-of-the-art climate models that provide ensembles of simulations with and without the effect of anthropogenic forcings, and, using the simulated temperatures at Kyoto, we obtain representations of the cherry flowering season under different climatic conditions. An observationally-based correction is also applied to the simulated temperatures to introduce the effect of urban warming. We find a significant anthropogenic shift in the mean flowering season of over a week, about half of which is due to urban warming. By the end of the century and under medium emissions, the early shift is estimated to further increase by almost a week. Extremely early flowering dates, as in 2021, would be rare without human influence, but are now estimated to be 15 times more likely, and are expected to occur at least once a century. Such events are projected to occur every few years by 2100 when they would no longer be considered extreme.

## 1. Introduction

Cherry blossom is celebrated as the most iconic herald of spring in several cultures. Given its fleeting appearance, understanding its timing is critical in countries like Japan and South Korea, where spring festivals are vital to the local economy [1]. A warming climate leads to earlier flowering times and poses a challenge to predictability [2–11]. Besides tourism, the sensitivity of tree phenology to rising temperatures would also have knock-on effects on crop-tree farming and land management practises [12–14]. The latest scientific report of the Intergovernmental Panel on Climate Change (IPCC) concluded it is virtually certain that human influence has been a major driver of the observed warming in many sub-continental regions [15]. Moreover, attribution studies have given evidence of a lengthening of the growing season driven by human influence with impacts on vegetation [16–18]. These studies may indeed suggest a link between anthropogenic warming and cherry flowering, but there is still a missing step in attribution research that would establish in a more direct manner the effect of human influence on blossom times. The lack of such a direct approach is noted not only in phenology studies but more generally in impacts attribution research, and largely stems from limited collaboration between impacts and attribution experts. Here we aim to fill this gap by presenting such an end-to-end attribution analysis, which assesses the changing risk of past and future extreme shifts in Kyoto's cherry blossom season driven by human activity.

Phenological studies of Kyoto's cherry trees benefit from a long record of full flowering dates (FFDs) that goes back to 812 AD. The record has been compiled from imperial court diaries and chronicles, with gaps being filled between updates as more data became available, and has been extended to the present with routine phenological observations in more recent times [19–22]. Unlike proxy data that rely on dating procedures, Kyoto's phenological data facilitate a more precise reconstruction of past climates [23]. While Kyoto's long FFD record is now well-established in scientific literature, it has not yet been integrated into an attribution assessment that would partition FFD changes between natural and anthropogenic climatic drivers. Besides this new perspective, our study also applies for the first time a probabilistic attribution methodology to a phenological impact, in order to assess the changing likelihood of FFD extremes due to human influence. Timeseries of the Kyoto's FFDs (figure 1(a)) illustrate large inter-annual variations, but also a gradual move of peak flowering in recent decades from late to early April. This move would be expected to increase the likelihood of extremely early FFDs and, consistent with that expectation, the earliest FFD in Kyoto's multi-centennial record was observed on the 26th of March 2021. To what extent can historical FFDs changes be attributed to anthropogenic forcings and how do these forcings alter the present and future risk of extreme events like in year 2021? To address these questions, we adopt an interdisciplinary approach that firstly derives simulated FFDs with a phenological model, and subsequently conducts an attribution analysis to assess the effect of human influence. We employ the risk-based attribution framework [24] to infer changes in the flowering season based on large ensembles of climate model simulations with and without the effect of human influence.

## 2. Data and methods

### 2.1. FFD and temperature observations

In addition to the long FFD record we also use temperature observations at Kyoto's Meteorological Observatory during the instrumental period 1881–2021. Details on the FFD and temperature data are given in supplementary appendix 1 (available online at stacks.iop.org/ERL/17/054051/mmedia). Kyoto's FFDs are highly anti-correlated with the mean temperature in March, as illustrated in figure 1(b) (correlation coefficient of $-0.85$). A warming trend since the mid-20th century maps onto cherry tree phenology, as flowering times arrive earlier. Attribution research has demonstrated the significant role of anthropogenic forcings in rising mean and extreme temperatures in East Asia [25–28], primarily driven by greenhouse gas emissions. In Kyoto, in addition to greenhouse gases, the effect of urbanisation is also expected to be an important contributor to the warming [29].

To illustrate the urban effect (figure 2(a)) we compare Kyoto's temperature timeseries with those from the rural station of Kameoka in the north-western suburbs of Kyoto. It is evident that the originally almost identical timeseries begin to diverge after the 1940s when the city's urban expansion took off. The temperature difference between the two locations (figure 2(b)) shows that the urban bias continues to increase until about the end of the 20th century, at which point Kyoto's observation station appears to be surrounded by a predominantly urbanised environment. The temperature difference between the two stations smoothed with 30 year running means (red line in figure 2(b)) to minimise the effect of internal variability is used for the urban-correction of simulated temperatures, as we will explain later. The difference is also extended to future years, assuming the urban warming has already reached its peak. It should be noted that the urban warming plotted in figure 2(b) corresponds to the mean temperature from February to April, as the phenological model uses daily temperature data from mainly these three months. However, we find that the urban effect does not notably vary between individual months, as illustrated, for example, in supplementary figure 1 for the month of March.

### 2.2. The CMIP6 ensembles

We conduct the attribution analysis with a suite of 14 models which contributed to the Coupled Model Intercomparison Project Phase 6 (CMIP6) Project [30] (supplementary table 1). We select all models that provide daily and monthly mean temperature data for two experiments, one with and one without human influence on the climate [31]. The former experiment (ALL) includes all external climatic forcings, i.e. changes in well-mixed greenhouse gases, aerosols, ozone and land use, as well as natural forcings that represent changes in volcanic aerosols and the solar irradiance. The second experiment (NAT) describes a hypothetical world without human influence on the climate and so includes natural forcings only. The models provide multiple ALL and NAT simulations and, to avoid giving high weight to models with larger ensembles, we limit the number of simulations used in the study to a maximum of 10 per model for each experiment. In summary, the daily data are derived from 51 ALL and 55 NAT simulations, while larger ensembles are available for monthly data (supplementary table 1). Both experiments start in year 1850, and we also consider future changes by extending the ALL simulations to the end of the 21st century with the 'middle of the road' Shared Socioeconomic Pathway 2 4.5 (SSP2 4.5) [32], a scenario that describes a plausible pathway given the current mitigation efforts [33].

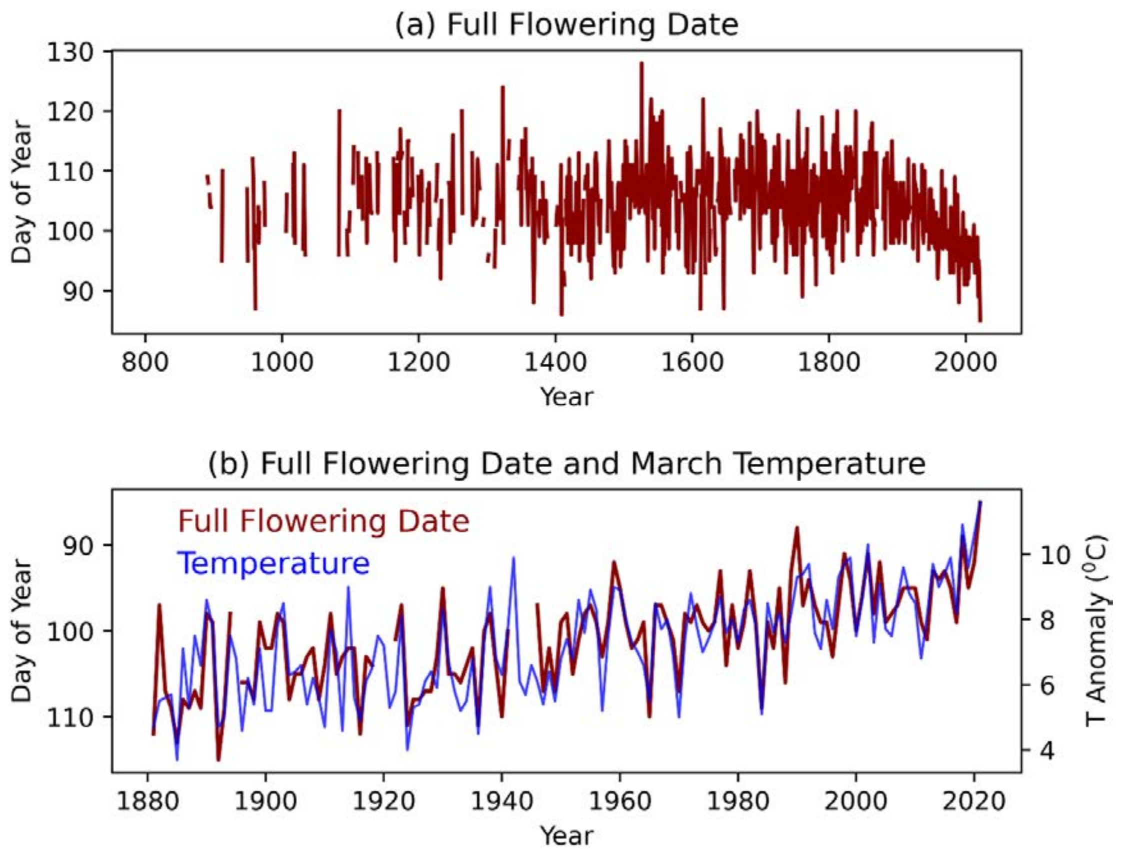


**Figure 1.** Observed FFDs and March temperatures in Kyoto. (a) Timeseries of observed FFDs since year 812 AD. (b) Timeseries of observed mean March temperatures during 1881–2021 (blue) plotted together with the FFD timeseries for the same period (red). The $y$-axis of the temperature timeseries is inversed to help visualise the relationship with the FFD. The record temperature and FFD both fall in year 2021 (last year in the timeseries).

For each model we extract temperature data at the grid-point located closest to Kyoto (35N, 135.7E). Although temperature spatial correlations are large enough to justify this approximation, the models have a relatively coarse horizontal resolution, of the order of a few hundred kilometres, which represents the wider rural area around the city rather than the urban environment where the FFD and temperature records are collected. Indeed, we find that the ALL simulations yield trends lower than the observed trend in Kyoto, but consistent with the lower trend in Kameoka (figure 2(c)). To account for the urban effect, we add the observationally estimated urban warming (red line in figure 2(b)) to temperature data from the ALL experiment. The urban correction is not applied to the NAT temperatures, as the natural climate is not influenced by any human forcings. Modelled temperatures also have mean biases relative to the observations, which are typically corrected by ensuring that the mean simulated temperature over a baseline period agrees with the observations[34]. Here we use the first 50 years of the observational period as a baseline (1881–1930), as it is long enough to provide a reliable bias estimate, but also early enough not to be considerably influenced by anthropogenic warming. We estimate the mean February to April temperature over the baseline years from the ALL simulations of each model and subtract it from the equivalent observed mean. We then remove this estimated bias from both the ALL and NAT simulations of the same model and repeat the procedure for all the models. The mean correction factor (supplementary table 2) is again found not to vary appreciably between months and, assuming it is constant, we also apply it to simulated daily temperatures between February and April. The ALL trends from bias-corrected data that also include urban warming are consistent with the observations (figure 2(d)) and the ensemble mean trend agrees well with the observed trend in Kyoto after correction.

### 2.3. Model evaluation

As attribution results are derived from model experiments, it is essential to demonstrate that our multi-model ensemble can reliably represent the main characteristics of Kyoto's March temperatures, which are closely linked to the FFDs. Apart from historical ALL trends, already shown to be consistent with the observations, we also employ here some additional standard evaluation assessments [34] to examine whether the modelled variability and temperature distribution compare well with the observations. March temperature timeseries are illustrated in figure 3(a). The ALL simulations reproduce the observed long term

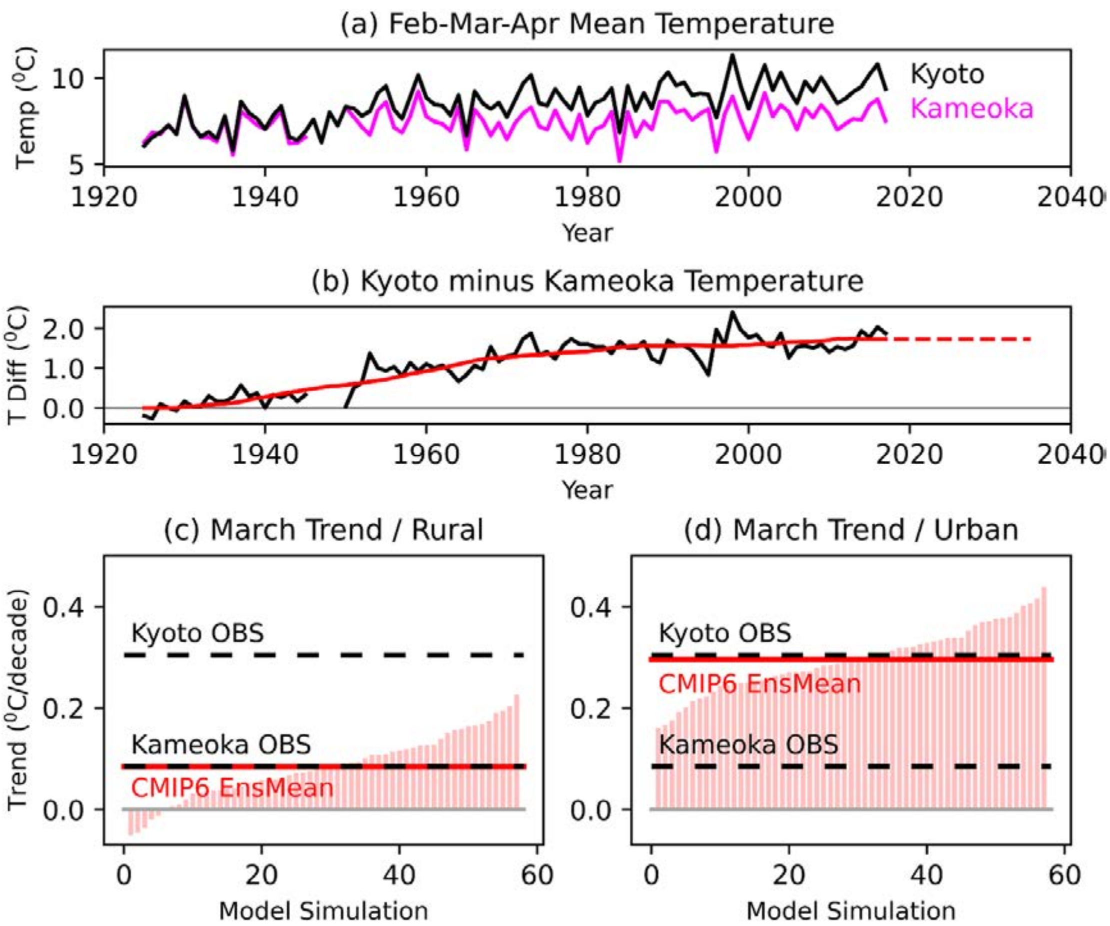


**Figure 2.** The influence of urbanisation on Kyoto's temperature. (a) Timeseries of the observed February to March mean temperature in Kyoto (black) and the rural area of Kameoka (purple). (b) The temperature difference between the two locations (black) and a smoothed version (red) produced with 30 year running means and extended to the future (dashed red line). (c) March temperature trends from the individual ALL simulations over the period 1925–2017 without the urban correction (vertical pink bars), the ensemble mean trend (horizontal red line), and the observed trends in Kyoto and Kameoka (black horizontal dashed lines). (d) Same as panel d, but for model data corrected to include the urban warming.

warming, projected to continue in future decades. On the other hand, the NAT climate appears to be largely stationary, suggesting that Kyoto's warming trend is of anthropogenic origin. Variability over different timescales is commonly assessed with power spectra [34, 35]. Spectra from detrended temperature timeseries show that the observations lie within the range of the models (figure 3(b)). Finally, using the quantile–quantile plot (figure 3(c)) we affirm that the temperature distribution constructed with the ALL ensemble (both main body and tails) is in overall agreement with the observations. We therefore conclude that the CMIP6 data employed here are fit for the purposes of the attribution analysis. Evaluation assessments applied to the data without the urban effect correction also confirm that the models represent well the rural temperatures of Kameoka (supplementary figure 2).

### 2.4. Phenological modelling

Phenological modelling of blooming dates ranges from simple regression methods to more sophisticated physical-based models like the growing degree days phenological models [36–39]. The latter represent the transition from a rest period to a forcing period when heat units are accumulated until a predefined heating requirement is met. Here we employ the Days Transformed to Standard temperature (DTS) model [40–42], an alternative accumulation model that proposes an exponential contribution of the daily temperature on growth during the development process. The DTS value for day $j$ in year $i$, $\mathrm{DTS}_{ij}^{\mathrm{day}}$, corresponds to the amount of daily growth at temperature $T_{ij}$ relative to the to the growth at a standard temperature $T_s$ and is approximated by the relationship:

$$\mathrm{DTS}_{ij}^{\mathrm{day}} = \exp\left[\frac{E_\alpha (T_{ij} - T_s)}{R \cdot T_{ij} \cdot T_s}\right]. \tag{1}$$

The parameter $E_\alpha$ (J mol$^{-1}$) describes the response of flower buds to temperature, and $R$ is the universal gas constant (8.314 J mol$^{-1}$ K$^{-1}$). The FFD is estimated as the day when the accumulation of daily DTS values, after a starting date $D$, reaches the

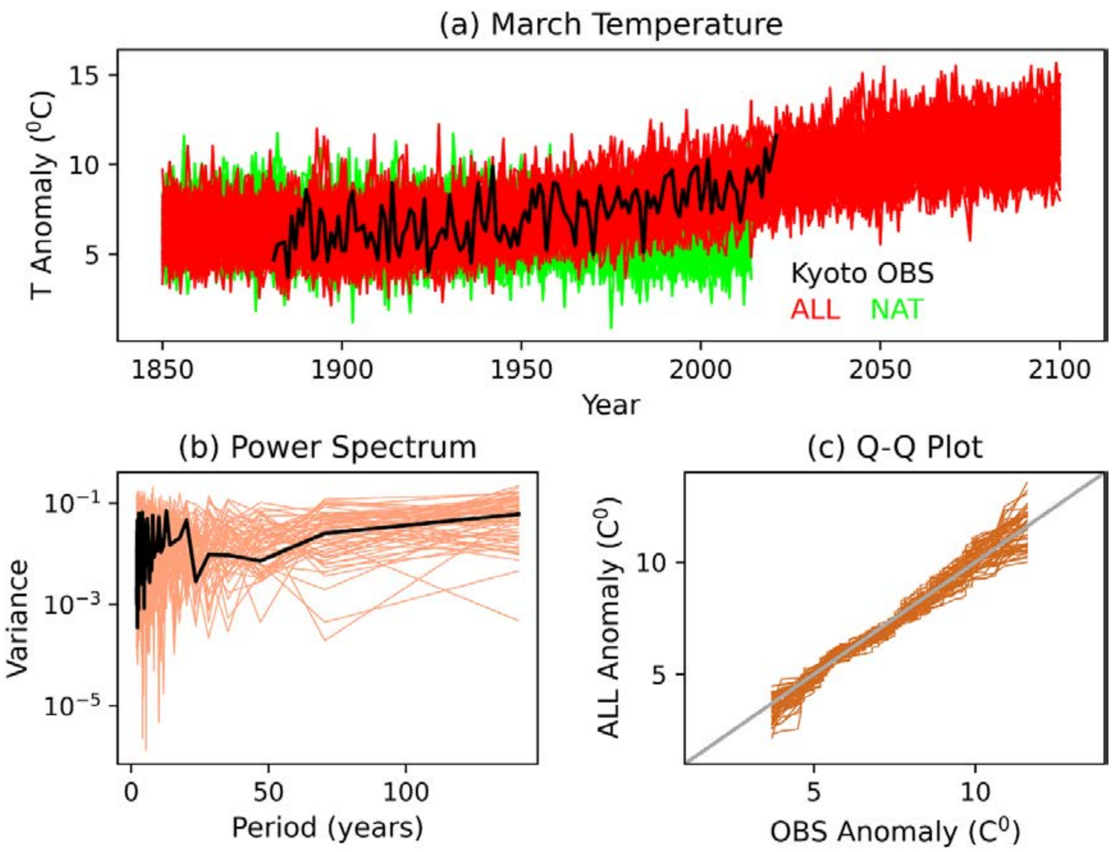


**Figure 3.** Simulated March temperature at Kyoto and model evaluation. (a) Timeseries of Kyoto's March temperature from observations (black line), and CMIP6 simulations with all external forcings (red lines) and natural forcings only (green lines). The simulations of the ALL experiment are extended to 2100 with SSP2 4.5. The modelled temperatures are bias-corrected, and the ALL temperatures include the effect of urban warming. (b) Power spectra from detrended timeseries of the March mean temperature over the period 1881–2021 computed with observations (black) and model simulations (orange). (c) Quantile-quantile (Q–Q) plots for each of the 51 ALL simulations, comparing the simulated and the observed March temperature in Kyoto over the observational period.

mean accumulation value over a calibration period with $N$ years:

$$\mathrm{DTS}^{\mathrm{calib}} = \frac{1}{N}\sum_{i=1}^{N}\sum_{j=D}^{B_i}\mathrm{DTS}_{ij}^{\mathrm{day}} \quad (2)$$

where $B_i$ denotes the FFD in year $i$. The parameters of the DTS model for Kyoto's cherry trees were estimated in previous work by an error analysis [41] for the 30 year calibration period 1911–1940 ($N = 30$), when the influence of urban and other anthropogenic warming is small. The parameter values, also used in this study, are $E_\alpha = 56$ kJ mol$^{-1}$ and $D = 42$ (11 February), while the mean DTS over the calibration period is $\mathrm{DTS}^{\mathrm{calib}} = 32.75$. Applying the DTS model to daily temperature data from the ALL and NAT simulations we calculate FFD values for all the simulated years.

### 2.5. Attribution

Using the FFD data derived from the ALL and NAT experiments, we first compute the change in the FFD relative to the natural climate in a reference time-window, e.g. a decade. To estimate the FFD change we use the $51 \times 10$ annual estimates of the FFD extracted from the 51 ALL simulations for the reference decade. Assuming the NAT climate is largely stationary, the mean FFD without anthropogenic climate change is approximated simply by the mean of the 9405 estimates derived from the NAT simulations (171 years during the period 1850–2020 $\times$ 55 simulations). We then subtract the mean NAT FFD from each of the 510 ALL estimates and compute the anthropogenic signal as the mean of the resulting 510 values. The associated uncertainty, representing year-to-year departures from the mean anthropogenic change because of internal climatic variations, is represented by the 5th and 95th percentiles of a normal distribution fitted to the same 510 values. The procedure is also applied to data from the ALL experiment but without the urban correction, to examine the what the anthropogenic influence would be in a rural environment.

In the second part of our attribution analysis, we estimate the probability of extreme events (FFD = 85 or less). The natural world probability is estimated by fitting a Generalised Pareto distribution (GPD) to the 9405 FFD estimates derived from the NAT simulations. For the ALL climate, we compute

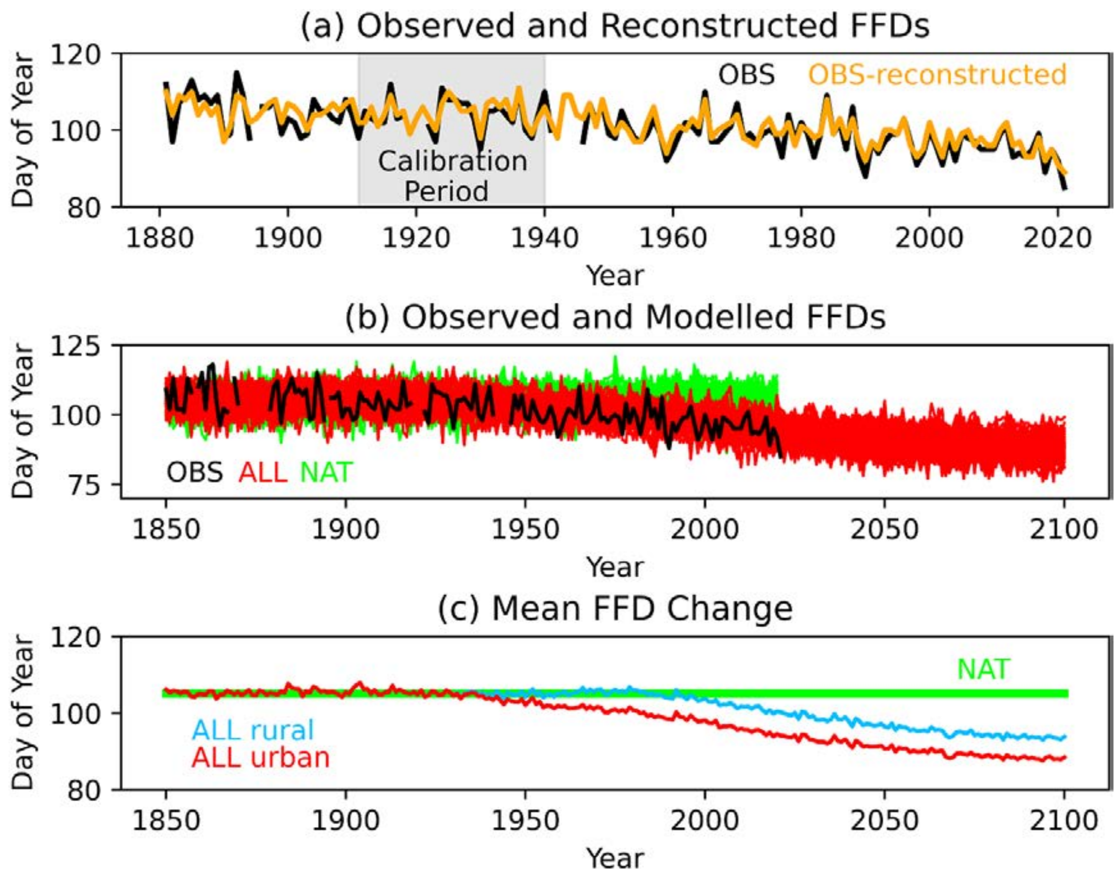


**Figure 4.** Kyoto's FFDs estimated with the DTS model. (a) Timeseries of observed FFDs (black) and FFDs reconstructed with the DTS model from Kyoto's daily temperature data (orange). The calibration period (1911–1940) used to derive the DTS parameters is marked by the grey area. (b) Timeseries of Kyoto's FFDs estimated with the DTS model using data from CMIP6 simulations with all external forcings (red) and natural forcings only (green). The observational FFD timeseries are also shown in black. (c) The mean of the 51 FFD timeseries from the ALL experiment (red) and the same estimated with ALL data that do not include urban warming (light blue). The NAT mean FFD is marked by the green line.

the probabilities in 20 year rolling windows, from the present climate to the end of the century. In this case we use the ALL FFDs in time windows 2012–2031, 2013–2023, …, 2081–2100, i.e. samples of 1020 values per time window. The ALL probabilities are also estimated for rural conditions in the same way from data that do not include the urban correction. Rural probabilities are also computed with the GPD, whereas the larger probabilities with the urban effect included are estimated with the normal distribution [43]. Uncertainties from sampling limitations are estimated with a Monte Carlo bootstrap procedure [43] that performs random resampling of the FFD estimates and recalculates the probability with the resulting alternative samples. The procedure is repeated 1000 times and the 5%–95% uncertainty range is then computed from the 1000 probability estimates.

## 3. Results

### 3.1. FFDs derived from the DTS model

Reconstructions of Kyoto's FFDs with the DTS model using daily temperature observations as input are in close agreement with the observed FFDs (figure 4(a)). The correlation coefficient between the reconstructed and observed FFD timeseries is 0.91 and the root mean square error is 2.5 d. The DTS model was calibrated over the period 1911–1940 and it is assumed that the estimated model parameters remain unchanged with time. This is an important assumption given the non-stationarity of the climate and the associated earlier occurrence of the FFDs with rising temperatures. It is evident, however, that the DTS model performs well outside its calibration period (figure 4(a)), with no degeneration in recent decades when the major shift towards earlier FFDs takes place. The good level of agreement between observed and reconstructed FFDs suggests that the DTS model does not introduce notable uncertainty in our analysis.

Timeseries of observed and model-based FFDs are illustrated in figure 4(b). As there is no long-term change in the NAT climate, FFDs as early as in 2021 are rare. However, even without anthropogenic forcings, such rare events may still take place because of internal variability, and we find 6 years with FFDs in late March out of the 9405 years provided by the NAT simulations. To illustrate the mean shift of the

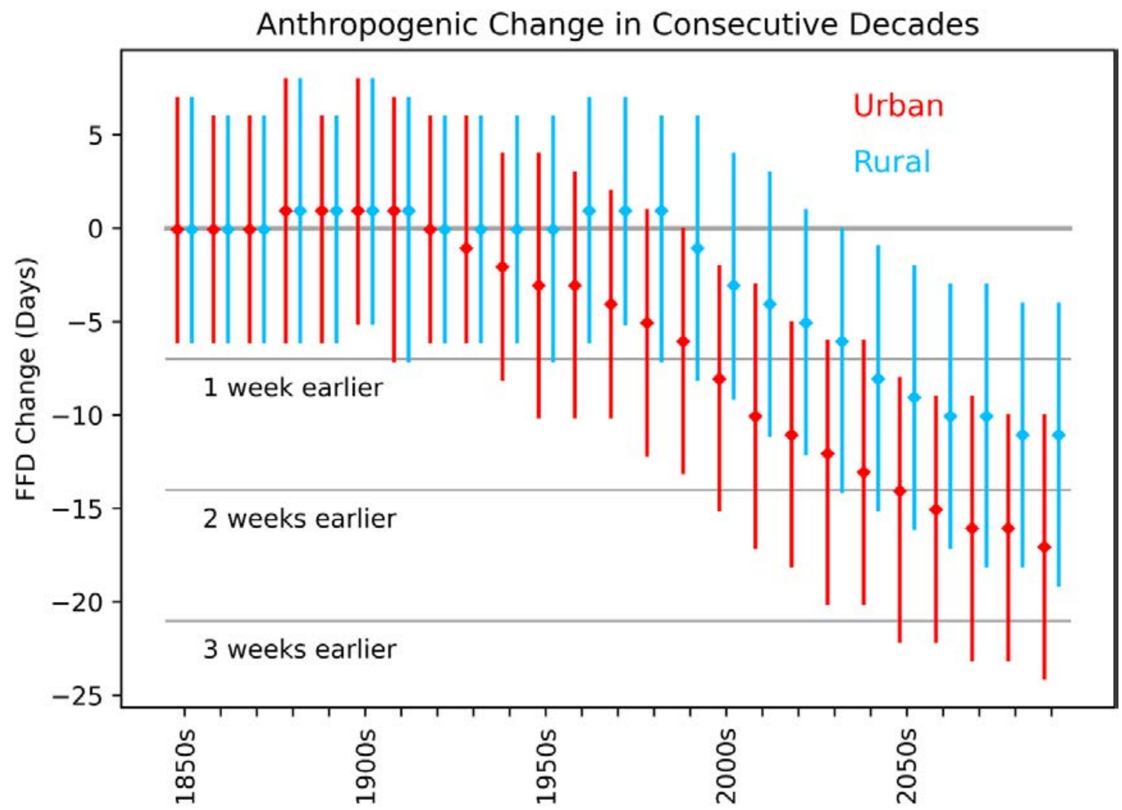


**Figure 5.** Anthropogenic influence on Kyoto's flowering season. The estimated FFD change in consecutive decades relative to a hypothetical natural climate without anthropogenic forcings computed with (red) and without (light blue) the effect of urban warming. The diamonds mark the mean FFD change and the vertical bars the expected year-to-year departures from the mean change due to internal variability. Shifts in the FFD by multiples of weeks are indicated by the horizontal grey lines.

flowering season with time we next plot the mean of the 51 ALL timeseries, for which much of the variability effect is removed (red line in figure 4(c)). We also compare the change in Kyoto with what it would have been without urban warming, using the ALL data but without the urban bias correction (light blue line). The figure also shows the mean FFD in the NAT climate calculated as the average of all the NAT year estimates (green line). Both urban and rural timeseries are consistent with the natural mean FFD in earlier decades but begin to diverge in later years towards earlier flowering seasons. Interestingly, the change comes several decades earlier in an urban setting, highlighting the importance of urban forcing on local scales. We will next quantify the anthropogenic contribution to changes in the FFD and will demonstrate a human-caused increase in the risk of extreme events like in year 2021.

### 3.2. Attributing changes in consecutive decades

We compute the change in the FFD relative to the natural climate in consecutive decades from 1850 to the end of the 21st century (figure 5) following the method in section 2.4. The mean change (diamonds in figure 5) provides a measure of the total anthropogenic effect on the FFDs and the 5%–95% range (vertical bars) represents interannual departures from the mean change due to internal variability. We find that after about the 1930s, human influence leads to earlier flowering, with an estimated shift of 11 d in the present climate and 17 d by 2100. The anthropogenic effect is detectable in the present decade above internal variability, as the range of the FFD change no longer encompasses zero. Without urban warming, the anthropogenic signal would emerge several decades later, at around the end of the 20th century, and would lead to a smaller shift of 5 d at present and 11 d by 2100. Hence, in a rural setting, the current anthropogenic change in Kyoto's flowering season would not be observed until the end of the century. Our results also indicate a slowdown in the shift of the FFDs during the course of this century, though the precise trajectory of future changes depends on the selected emissions scenario. We expect the human impact would be further reduced in a more sustainable development pathway than the middle-of-the-road SSP2 4.5, which stresses the importance of lowering greenhouse gas emissions.

### 3.3. The changing likelihood of extreme FFDs

Risk-based attribution studies estimate the changing likelihood of extreme events from ensembles of simulations that represent different climatic conditions. Applying the same approach here, we construct probability distributions of the FFD for the present climate, the climate of the late 21st century

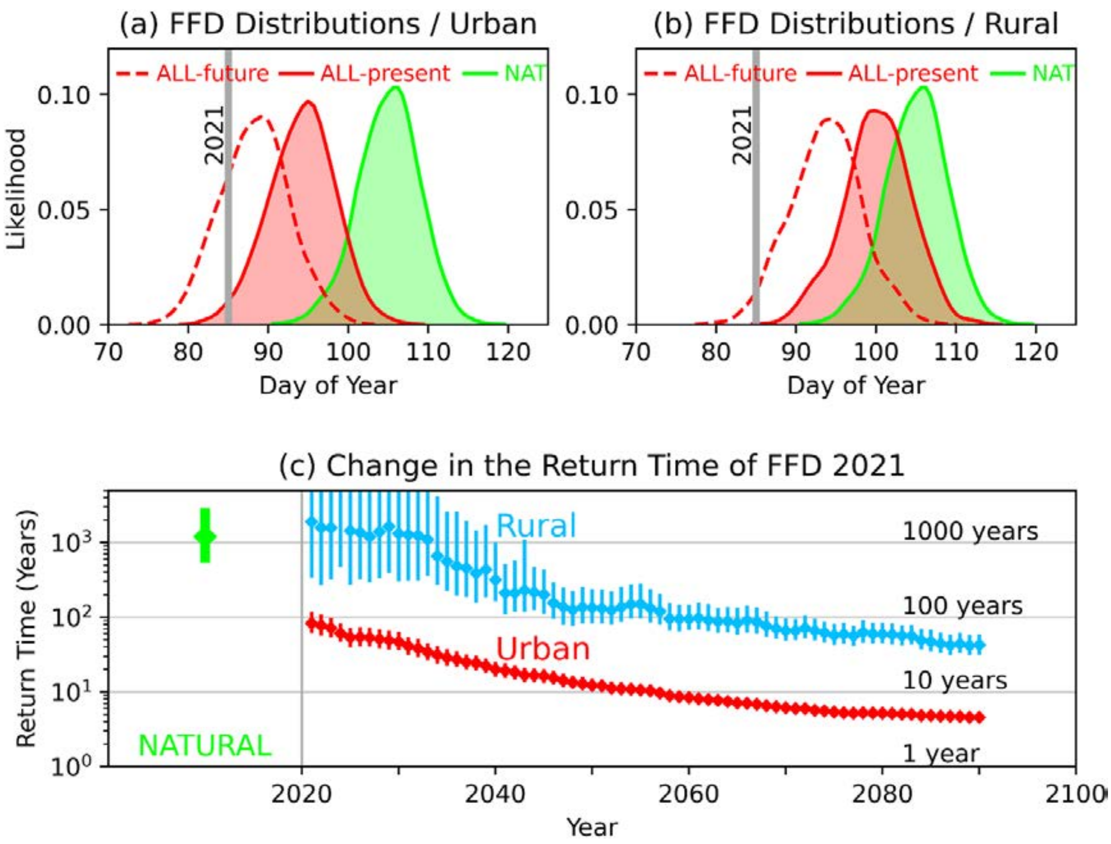


**Figure 6.** Anthropogenic influence on the likelihood of extremely early flowering. (a) Normalised distributions of Kyoto's FFD constructed with data from CMIP6 experiments that correspond to the natural climate (green line), the present-day climate of 2012–2031 (red solid line) and the climate of the late century 2081–2100 (dashed red line). The grey vertical line marks the extremely early FFD observed in 2021. (b) The same as panel a, but without the effect of urban warming in the ALL distributions. (c) The return time of extreme events with the FFD being at least as early as in 2021, estimated for the natural climate (green) and in 20 year rolling windows, from present-day to the end of the century, with (red) and without (light blue) urban warming. The best estimate of the return time is marked by the diamonds and the associated 5%–95% uncertainty range by the vertical bars.

and the natural climate without human influence (figure 6(a)). The present and future distributions are based on FFD data derived from the ALL experiment and extracted from two 20 year-periods used as a proxy of different climatic conditions, namely years 2012–2031, representing the climate of 2021 and of the present-day, and years 2081–2100, representing the late century. For the distribution of the natural world, we use all the FFD data from the NAT experiment. We also assess the effect of urban warming separately and construct distributions for rural conditions using data from the ALL experiment but without the urban correction (figure 6(b)). It is evident that the 2021 FFD would be extremely rare in the pre-industrial world as it lies well outside the main body of the NAT distribution. Without urban warming, the 2021 event would be more likely in today's climate, but still uncommon as it is positioned in the far tail of the rural distribution. However, the combined effect of urban and other anthropogenic warming has moved the distribution further towards earlier FFDs, increasing the likelihood of the 2021 record, while by 2100 the event lies much closer to the peak of the urban distribution and would therefore no longer be considered extreme.

Following the method described in section 2.4, we next calculate the likelihood of extremely early FFDs in the natural world and in 20 year rolling windows from present-day to the end of the century (figure 6(c)). The return time (inverse probability) of extremely early FFDs in the natural climate is estimated to be 1200 years (uncertainty range: 620–2500). The shift of the FFD in a climate influenced by anthropogenic forcings except urban warming is still largely influenced by variability (figure 5, present-day range includes zero) and so the return time of extremely early events encompasses the NAT range (figure 6(c)). The FFD sample used to estimate the rural likelihood is also much smaller than the NAT sample and since the early flowering events considered here are very rare, the estimated return time uncertainty in the present-day climate is much larger compared to NAT. However, in Kyoto's warmer urban climate the anthropogenic signal has emerged more clearly, and the likelihood of extremes is estimated to have already increased 15 times (7–30) because of human influence, with the return time reduced to 83 years (65–110). As temperatures continue to rise, early flowering events are found to become very common by 2100 with a return time of 4.6 years (4.2–4.9). Their likelihood also increases in the rural climate, for which the return time at the end of the century is estimated to be 43 years (34–56). Our results suggest a rapid change in the likelihood of extremely early flowering dates in Kyoto attributed to human influence that also reflects an imminent change in our perception of climatological seasons.

## 4. Discussion

Attribution of climate change impacts has been receiving increasing attention, as direct information on impacts is more pertinent, e.g. for the purposes of effective adaptation planning, than assessments of the underlying climatological changes. The need to bring closer impacts and attribution research is evident in the most recent report of the IPCC's Working Group II, in which detection and attribution perspectives are included in its chapters [44]. Impacts research may adopt established attribution methodologies like the risk-based approach, which has been foundational in studies of extreme weather and climate events [45] and has demonstrated a significant anthropogenic influence on characteristics of several different types of extremes [46]. Extending the approach from meteorological events to their impacts, enables us to assess, for example, changes in heat-related mortality [47], energy consumption [48], or in the economic cost of catastrophic weather events like hurricanes [49]. Our study presents a new phenological application of risk-based attribution to early cherry flowering trends in Kyoto.

We demonstrate that Kyoto's cherry flowering season arrives on average 1–2 weeks earlier because of anthropogenic climate change, with a projected shift of an extra week by the end of the century under a medium emissions scenario. As a result, extremely early flowering like in year 2021 becomes increasingly common in a warming climate and may occur every few years by 2100, when it will no longer be classified as extreme. In common with other multi-model studies, our analysis is dependent on the available model data, a potential limitation that is sometimes referred to as an ensemble-of-opportunity[50], though evaluation against observational data indicates that the models utilised here simulate well Kyoto's climate characteristics important to this study. Such evaluation assessments have been recognised as important in model-based attribution studies[51]. Estimates of future changes are also tied to the choice of the emissions scenario [33, 52]. Results with the middle-of-the-road SSP suggest that larger emission reductions would be necessary to prevent phenological changes in rural suburbs of Kyoto reaching the levels we currently see in the city.

## 5. Conclusions

Earlier flowering has been a known phenological impact of climate change [41, 53]. Nevertheless, no attribution analysis had previously established the precise contribution of anthropogenic forcings, the detectability of their signal above internal variability, or their pivotal role in the changing likelihood of extreme FFD events. This largely stems from a gap in attribution research that has mainly focussed on trends in climate variables and changes in characteristic of weather extremes, rather than on impacts of climate change. The latter requires collaborative effort between different disciplines, to combine modelling of climate-dependent impacts with attribution methods and thus facilitate end-to-end attribution investigations [54]. Moreover, strong links need to be established, not only among researchers, but also between the scientists and stakeholders for whom attribution information may form a robust basis for decision-making. For example, our analysis can be part of the information that would guide Kyoto's effective adaptation to climate change, helping to prevent its adverse impacts on the local economy. Finally, our work may also serve as a template of future studies extended to other regions and species, that would provide a more complete view of phenological changes resulting from human activity.

## Data availability statement

The data that support the findings of this study are available upon reasonable request from the authors.

## Acknowledgments

NC and PAS were supported by the Met Office Hadley Centre Climate Programme funded by BEIS and Defra. We acknowledge the World Climate Research Programme, which coordinated and promoted CMIP6 and thank the contributing climate modelling groups for producing and making available their model output, the Earth System Grid Federation (ESGF) for archiving the data and providing access, and the multiple funding agencies who support CMIP6 and ESGF.

## ORCID iD

Yasuyuki Aono https://orcid.org/0000-0002-6950-4341

## References

[1] Sakurai R *et al* 2011 Culture and climate change: japanese cherry blossom festivals and stakeholders' knowledge and attitudes about global climate change *Biol. Conserv.* **144** 654–8

[2] Primack R B, Higuchi H and Miller-Rushing A J 2009 The impact of climate change on cherry trees and other species in Japan *Biol. Conserv.* **142** 1943–9
[3] Chung U, Kim J-H and Kim K-H 2016 Variation and uncertainty in the predicted flowering dates of cherry blossoms *Asia-Pac. J. Atmos. Sci.* **52** 509–18
[4] Paltineanu C and Chitu E 2020 Climate change impact on phenological stages of sweet and sour cherry trees in a continental climate environment *Sci. Hortic.* **261** 109011
[5] Chmielewski F M, Götz K P, Weber K C and Moryson S 2018 Climate change and spring frost damages for sweet cherries in Germany *Int. J. Biometeorol.* **62** 217–28
[6] Körner C and Basler D 2010 Phenology under global warming *Science* **327** 1461–2
[7] Stuble K L, Bennion L D and Kuebbing S E 2021 Plant phenological responses to experimental warming—a synthesis *Glob. Change Biol.* **27** 4110–24
[8] Ge Q, Wang H, Rutishauser T and Dai J 2014 Phenological response to climate change in China: a meta-analysis *Glob. Change Biol.* **21** 265–74
[9] Amano T, Smithers R J, Sparks T H and Sutherland W J 2010 A 250-year index of first flowering dates and its response to temperature changes *Biol. Sci.* **277** 1693
[10] Bartolini S, Massai R, Iacona C, Guerriero R and Viti R 2019 Forty-year investigations on apricot blooming: evidences of climate change effects *Sci. Hortic.* **244** 399–405
[11] Drkenda P *et al* 2018 Comparison of climate change effects on pome and stone fruit phenology between Balkan countries and Bonn/Germany *Erwerbs-Obstbau* **60** 295–304
[12] Menzel A *et al* 2020 Climate change fingerprints in recent European plant phenology *Glob. Change Biol.* **26** 2599–612
[13] Moretti C L, Mattos L M, Calbo A G and Sargent S A 2010 Climate changes and potential impacts on postharvest quality of fruit and vegetable crops: a review *Food Res. Int.* **43** 1824–32
[14] Menzel A, von Vopelius J, Estrella N, Schleip C and Dose V 2006 Farmers' annual activities are not tracking the speed of climate change *Clim. Res.* **32** 201–7
[15] Doblas-Reyes F J *et al* 2021 Linking global to regional climate change *Climate Change 2021: The Physical Science Basis. Contribution of Working Group I to the Sixth Assessment Report of the Intergovernmental Panel on Climate Change* V Masson-Delmotte *et al* ed (Cambridge: Cambridge University Press) pp 1363–512
[16] Christidis N, Stott P A, Brown S, Karoly D J and Caesar J 2007 Human contribution to the lengthening of the growing season during 1950–1999 *J. Clim.* **20** 5441–54
[17] Xu L *et al* 2013 Temperature and vegetation seasonality diminishment over northern lands *Nat. Clim. Change* **3** 581–6
[18] Chen C, Li T, Sivakumar B, Li J and Wang G 2020 Attribution of growing season vegetation activity to climate change and human activities in the Three-River headwaters region, China *J. Hydroinf.* **22** 186–204
[19] Taguchi T 1939 Climatic change in historical time in Japan *J. Mar. Meteorol. Soc.* **19** 217–27
[20] Sekiguchi T 1969 The historical dates of Japanese cherry festival since the 8th century and her climatic changes *Tokyo Geog. Pap.* **13** 175–90
[21] Aono Y and Omoto Y 1993 Variation in the March mean temperature deduced from cherry blossom in Kyoto since the 14th century *J. Agric. Meteorol.* **48** 635–8
[22] Aono Y and Omoto Y 1994 Estimation of temperature at Kyoto since 11th century using flowering data of cherry tree in old documents *J. Agric. Meteorol.* **49** 263–72
[23] Aono Y and Saito S 2010 Clarifying springtime temperature reconstructions of the medieval period by gap-filling the cherry blossom phenological data series at Kyoto, Japan *Int. J. Biometeorol.* **54** 211–9
[24] Stott P A *et al* 2016 Attribution of extreme weather and climate-related events *WIREs Clim. Change* **7** 23–41
[25] Zhai P, Zhou B Q and Chen Y 2018 A review of climate change attribution studies *J. Meteorol. Res.* **32** 671–92
[26] Stott P A 2003 Attribution of regional-scale temperature changes to anthropogenic and natural causes *Geophys. Res. Lett.* **30** 1728
[27] Dong S *et al* 2018 Observed changes in temperature extremes over Asia and their attribution *Clim. Dyn.* **51** 339–53
[28] Christidis N, Stott P A and Zwiers F W 2015 Fast-track attribution assessments based on pre-computed estimates of changes in the odds of warm extremes *Clim. Dyn.* **45** 1547–64
[29] Iizawa I *et al* 2016 Time evolution of an urban heat island from high-density observations in Kyoto city *Sola* **12** 51–54
[30] Eyring V *et al* 2016 Overview of the coupled model intercomparison project phase 6 (CMIP6) experimental design and organization *Geosci. Model Dev.* **9** 1937–58
[31] Gillett N P *et al* 2016 The detection and attribution model intercomparison project (DAMIP v1.0) contribution to CMIP6 *Geosci. Model Dev.* **9** 3685–97
[32] Riahi K *et al* 2017 The shared socioeconomic pathways and their energy, land use, and greenhouse gas emissions implications: an overview *Glob. Environ. Change* **42** 153–68
[33] Hausfather Z and Peters G P 2020 Emissions—the 'business as usual' story is misleading *Nature* **577** 681–620
[34] Christidis N, McCarthy M and Stott P A 2020 The increasing likelihood of temperatures above 30–40 °C in the United Kingdom *Nat. Commun.* **11** 3093
[35] Gillett N, Allen M R and Tett S F B 2000 Modelled and observed variability in atmospheric vertical temperature structure *Clim. Dyn.* **16** 49–61
[36] Cesaraccio C, Spano D, Snyder R L and Duce P 2004 Chilling and forcing model to predict bud-burst of crop and forest species *Agric. For. Meteorol.* **126** 1–13
[37] Kwon E-Y, Jung J-E, Chung U, Yun J I and Park H S 2008 Using thermal time to simulate dormancy depth and bud-burst of vineyards in Korea for the twentieth century *J. Appl. Meteorol. Climatol.* **47** 1792–801
[38] Chung U, Jung J-E, Seo H-C and Yun J I 2009 Using urban effect corrected temperature data *Clim. Change* **93** 447–63
[39] Chuine I and Régnière J 2017 Process-based models of phenology for plants and animals *Annu. Rev. Ecol. Evol. Syst.* **48** 159–82
[40] Konno T and Sugihara S 1986 Temperature index for characterizing biological activity in soil and its application to decomposition of soil organic matter *Bull. Natl Inst. Agro-Environ. Sci.* **1** 51–68
[41] Aono Y and Kazui K 2008 Phenological data series of cherry tree flowering in Kyoto, Japan, and its application to reconstruction of springtime temperatures since the 9th century *Int. J. Climatol.* **28** 905–14
[42] Aono Y and Murakami N 2017 A simplified method to estimate cherry blossom phenology considering temperature during endodormancy process *Clim. Biosphere* **17** 25–33
[43] Christidis N *et al* 2013 A new HadGEM3-A based system for attribution of weather and climate-related extreme events *J. Clim.* **26** 2756–83
[44] IPCC 2022 Climate change 2022: impacts, adaptation, and vulnerability *Contribution of Working Group II to the Sixth Assessment Report of the Intergovernmental Panel on Climate Change* H-O Pörtner *et al* ed (Cambridge: Cambridge University Press) (In Press)
[45] Seneviratne S I *et al* 2021 Weather and climate extreme events in a changing climate *Climate Change 2021: The Physical Science Basis. Contribution of Working Group I to the Sixth Assessment Report of the Intergovernmental Panel on Climate Change* V Masson-Delmotte *et al* ed (Cambridge: Cambridge University Press) pp 1513–765
[46] Herring S C, Christidis N, Hoell A, Hoerling M P and Stott P A Eds 2022 Explaining extreme events of 2020 from a climate perspective *Bull. Am. Meteorol. Soc.* **103**
[47] Vicedo-Cabrera A M *et al* 2021 The burden of heat-related mortality attributable to recent human-induced climate change *Nat. Clim. Change* **11** 492–500
[48] Christidis N, McCarthy M and Stott P A 2021 Recent decreases in domestic energy consumption in the United

Kingdom attributed to human influence on the climate *Atmos. Sci. Lett.* **22** e1062
[49] Frame D J, Wehner M F, Noy I and Rosier S M 2020 The economic costs of hurricane Harvey attributable to climate change *Clim. Change* **160** 271–81
[50] Stone D, Allen M R, Selten F, Kliphuis M and Stott P A 2007 The detection and attribution of climate change using an ensemble of opportunity *J. Clim.* **20** 514–6
[51] Otto F E L 2017 Attribution of weather and climate events *Annu. Rev. Environ. Resour.* **42** 627–46
[52] O'Neill B C *et al* 2020 Achievements and needs for the climate change scenario framework *Nat. Clim. Change* **10** 1074–84
[53] Chung U, Mack L, Yun J I and Kim S H 2011 Predicting the timing of cherry blossoms in Washington, DC and mid-Atlantic States in response to climate change *PLoS One* **6** e27439
[54] Perkins-Kirkpatrick S E *et al* 2022 On the attribution of the impacts of extreme weather events to anthropogenic climate change *Environ. Res. Lett.* **17** 024009